

## ***Supplementary Information***

### **Comprehensive biosensor integrated with ZnO nanorods FETs array for selective detection of glucose, cholesterol and urea**

Rafiq Ahmad<sup>a</sup>, Nirmalya Tripathy<sup>b</sup>, Jin-Ho Park<sup>c</sup> and Yoon-Bong Hahn<sup>a,\*</sup>

<sup>a</sup> School of Semiconductor and Chemical Engineering, and Nanomaterials Processing Research, Chonbuk National University, 567 Baekje-daero, Deokjin-gu, Jeonju 561-756, Republic of Korea

<sup>b</sup> Department of BIN Fusion Technology, Chonbuk National University, 567 Baekje-daero, Deokjin-gu, Jeonju 561-756, Republic of Korea

<sup>c</sup> Department of Veterinary Internal Medicine, College of Veterinary Medicine, Chonbuk National University, 567 Baekje-daero, Deokjin-gu, Jeonju 561-756, Republic of Korea

---

\* **Corresponding author.** Tel.: +82 63 2702439; fax: +82 63 2702306; E-mail: [ybhahn@chonbuk.ac.kr](mailto:ybhahn@chonbuk.ac.kr) (Y. B. Hahn)

#### **Table of contents**

1. Experimental details.....	S2
1.1. Fabrication of hybrid FET biosensor device.....	S2
1.2. Characterization.....	S3
2. TEM and XRD analysis of ZnO NRs.....	S4
3. Electrical properties of the seed layer and ZnO NRs i-FETs array before and after enzymes immobilization.....	S5
4. Investigation of working potentials range, pH change and effect of pH.....	S6
5. Selectivity test.....	S9
6. Stability test.....	S10
7. Mice whole blood samples analysis.....	S10
8. Diabetic dog blood samples analysis.....	S11
9. Table-S1: Determination of glucose, cholesterol and urea concentrations in mice whole blood samples.....	S12
9. Table-S2: Determination of glucose, cholesterol and urea concentrations in hypo- and hyperglycemic dog serum samples.....	S13
10. Reference.....	S14

## 1. Experimental details

### 1.1. Fabrication of hybrid FET biosensor device

The FETs array based biosensor was fabricated using a facile approach on a cleaned substrate (2×2cm) of Si(100)/SiO<sub>2</sub>(200 nm). Fig. S1 shows the schematic of fabrication process of ZnO NRs FETs array based biosensor. First, a thin PMMA layer of ~400 nm thickness was spin coated on the Si/SiO<sub>2</sub> and baked at 170 °C for 30 min, followed by an exposure to electron beam lithography for defining the three separate set of source-drain electrodes area (a,b).<sup>1</sup> After developing, a silver (Ag) layer of about 100 nm was deposited on lithographically defined area by sputtering and formed the electrode pads after lift-off process in acetone (c). The source-drain electrodes were designed to have the channel length of 0.5 cm. After that, similarly patterned regions were formed by lithography covering half of both ends of source-drain electrodes and leaving channel width of 0.1 cm (d). Then, three ZnO NRs arrays were grown by solution process after making a ZnO seed layer of 70-80 nm. A subsequent 1 h acetone soak was used to lift off the remaining photoresist, leaving well-defined areas of ZnO NRs arrays grown between source and drain on Si/SiO<sub>2</sub> (e,f). Before immobilization of enzymes (glucose oxidase (GOx), cholesterol oxidase

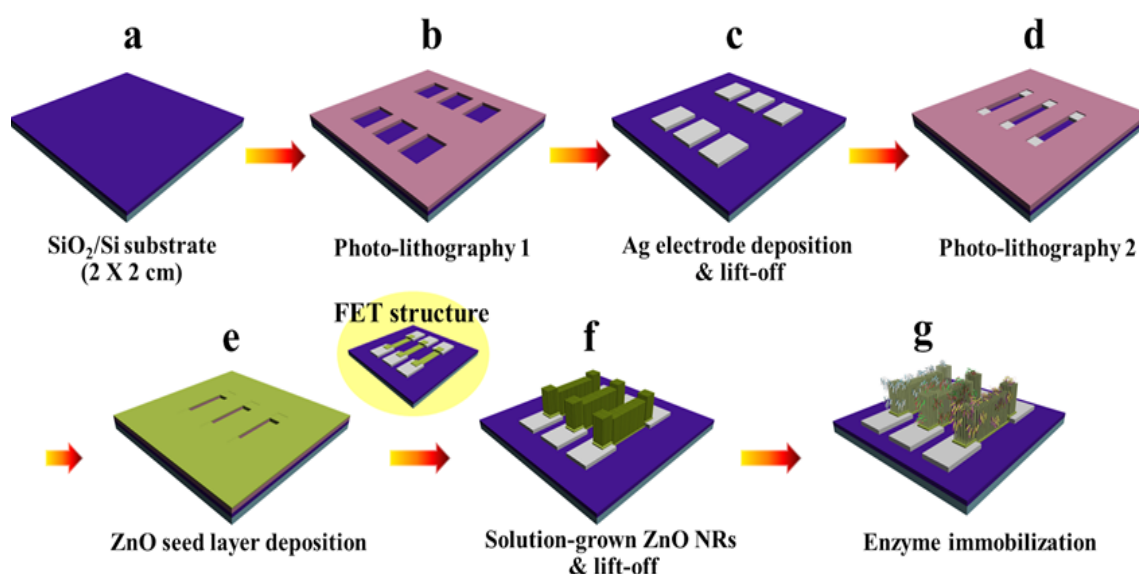


**Fig. S1** Schematic fabrication processes of ZnO NRs i-FETs hybrid biosensor electrodes: (a) Si/SiO<sub>2</sub> substrate, (b) photo-lithography 1 to define source/drain electrodes, (c) Ag deposition on Si/SiO<sub>2</sub> substrate by RF sputtering and lift-off the remaining photoresist, (d) Photo-lithography 2 to define areas for ZnO NRs growth, (e) ZnO seed layer deposition by RF sputtering, (f) growth of ZnO NRs arrays by bottom-up solution process and lift-off the remaining photoresist.

(ChOx) and urease (Ur)), the integrated biosensor having three ZnO NRs FETs arrays was double rinsed with PBS (0.1 M, pH 7.4, Sigma Aldrich) to generate hydrophilic surfaces. The enzyme solutions were prepared by dissolving GOx, ChOx and Ur (1.0 mg/mL each) in 0.1 M PBS (pH 7.4) and 5  $\mu$ L of each enzyme solution was immobilized onto the surface of ZnO NRs FETs array separately by a physical adsorption method (g). After dropping enzyme solutions on ZnO NRs i-FETs array separately, the device was kept at 4 °C for 12 h, which allowed enzymes to be absorbed onto the ZnO NRs surfaces. After drying at room temperature, the ZnO NRs i-FETs array biosensor was rinsed with DI water to remove extra enzymes. Finally, 1  $\mu$ L of 0.5 wt% Nafion solution was dropped onto the each enzyme immobilized ZnO NRs arrays surface to prevent possible enzyme leakage and avoid foreign interferences.

### ***1.2. Characterization***

The structural investigation of as-synthesized ZnO NRs was carried out by field emission scanning electron microscopy (FESEM, Hitachi S4700), transmission electron microscopy (TEM) and high-resolution TEM (HRTEM) equipped with digital charge-coupled device (JEOL-JEM-2010 equipped with CCD camera). The crystallinity of as-grown ZnO NRs was examined by X-ray diffraction (XRD, Rigaku) with Cu-K $\alpha$  radiation ( $\lambda=1.54178$  Å) in the range of 30-65° at 40 kV with 8°/min scanning speed. Moreover, the single crystallinity of the as-grown NRs was studied with selected area electron diffraction (SAED). The electrical properties of semiconducting ZnO NRs i-FETs array based biosensor were evaluated at room temperature under air-ambient conditions with a semiconductor parameter analyzer (HP 4155A) connecting fabricated biosensor with a data acquisition system for real-time data measurement. To determine the sensing properties of the fabricated biosensors, the drain current ( $I_D$ ) was measured with a fixed drain-source voltage ( $V_{DS} = 0.1$  V) while sweeping the different gate voltage range ( $V_G$ ). The  $V_G$  was applied via an Ag/AgCl reference gate electrode immersed in the solution. All sensing tests were performed in an ambient environment at room temperature. For comparing the biosensor efficiency, the concentration of analytes (glucose, cholesterol and urea) in mice blood, mice serum and diabetic serum samples were measured by using blood chemistry analyzer VetScan VS2 (Abaxis, Inc., Union City, CA 94587).

## 2. TEM and XRD analysis of ZnO NRs

The low- and high- resolution TEM images with SAED pattern of as-grown ZnO NR are shown in Fig. S2. The SAED pattern clearly delineates the fringes of ZnO (0001) planes with the interplanar spacing of 0.52 nm and confirms the single crystallinity with the preferential growth in [0001] direction. In the X-ray diffraction pattern measurement, a strongest peak at  $34.2^\circ$  attributed as ZnO (0002) confirming that the as-grown nanorods are grown along [0001] direction in preference, which is well-matched with high-resolution TEM and SAED analysis.

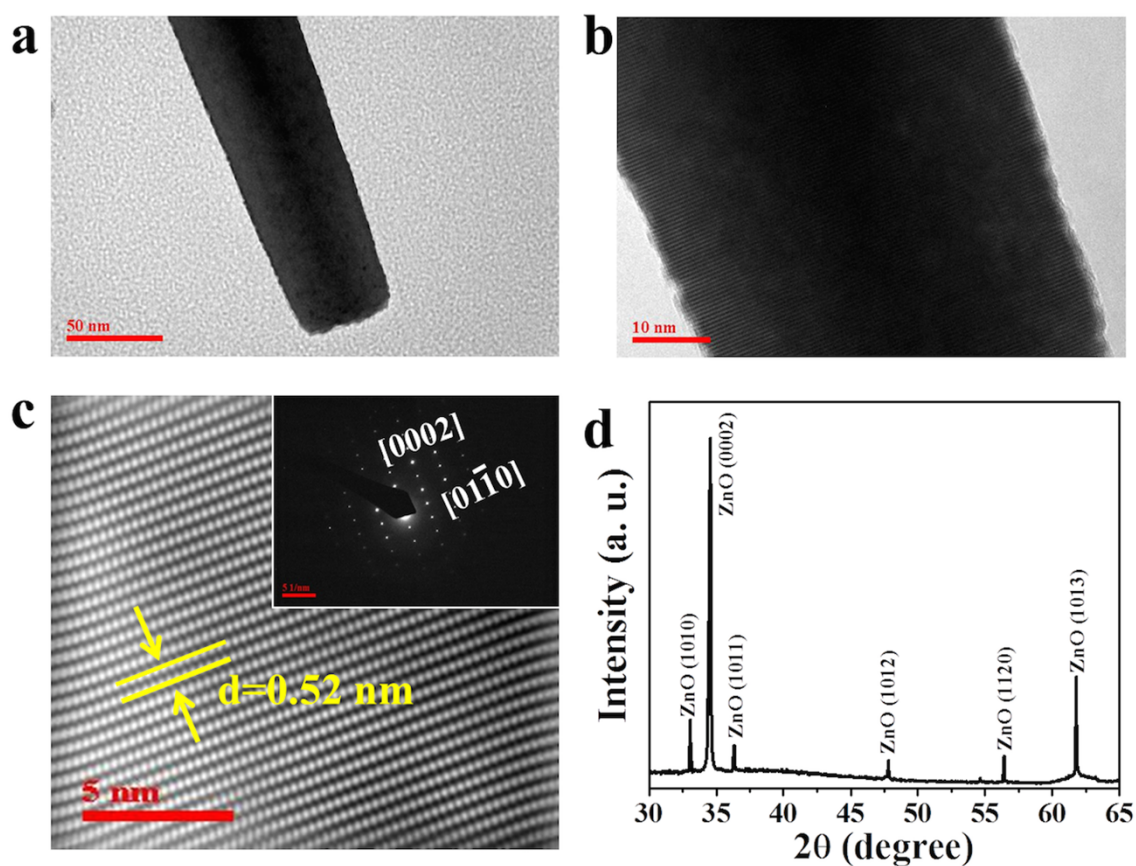


**Fig. S2** Low (a) and high (b) magnification TEM images, (c) HRTEM image (inset shows the SAED pattern) and (d) XRD pattern of ZnO NRs.

### 3. Electrical properties of the seed layer and ZnO NRs i-FETs array before and after enzymes immobilization

The electrical properties of the ZnO NRs i-FETs array before and after enzymes immobilization on ZnO NRs show an Ohmic contact with high slope (i.e.,  $di/dv$ ) values of 0.178, 0.177 and 0.176 nS for three ZnO NRs sensing arrays, respectively (Fig. S3a-c). A slight decrease in the slope was observed after enzymes immobilization. Nevertheless, after enzymes immobilization, the linearity in I-V characteristics was preserved and the  $di/dv$  values were also maintained within the same order of magnitude. Therefore, it can be considered that enzyme molecules are effectively immobilized on the ZnO NRs without any deterioration in electrical contact and conductivity. To ensure the electron conductance only from the ZnO NRs, we measured I-V characteristics from three samples of ZnO seed layer having thickness of 70-80 nm (Fig. S3d).

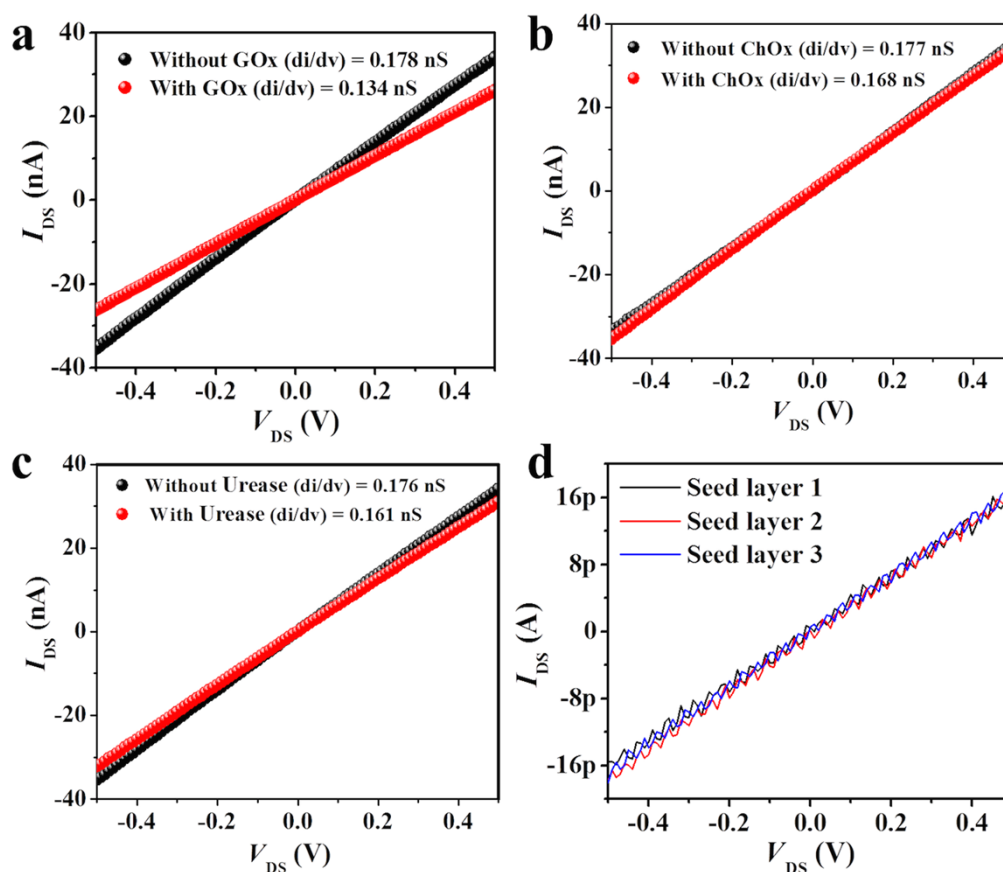


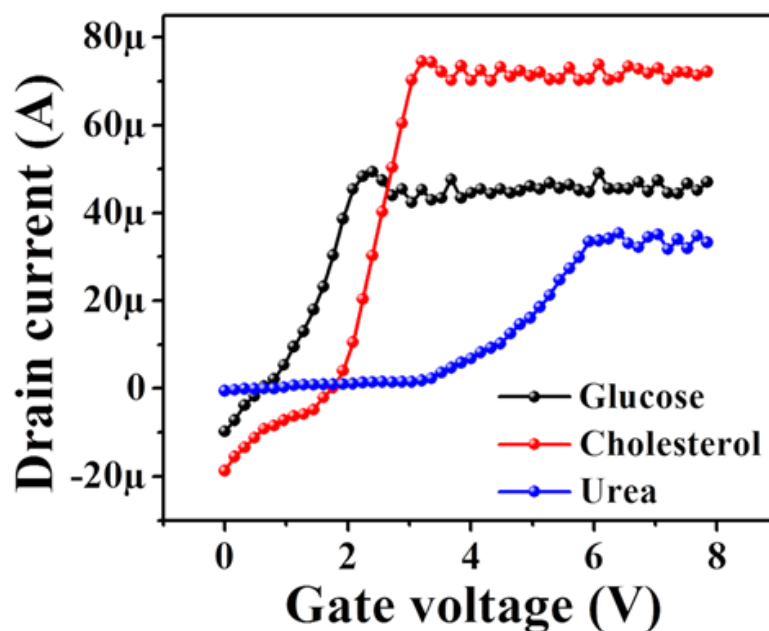
**Fig. S3** *I-V* characteristics of ZnO NRs FET-based hybrid biosensor device before and after enzyme immobilization at scan rate of 10 mVs<sup>-1</sup>. (a) GOx, (b) ChOx, (c) Urease and (d) Only sputtered ZnO seed layer.

#### **4. Investigation of working potentials range, pH change and effect of pH**

Further examinations were carried out to investigate the working potentials range, pH change with increasing concentrations of glucose, cholesterol and urea, and the effect of pH on the biosensor response. First, its working potential range was determined by  $I_D$ - $V_G$  (drain current versus gate voltage) characterization in the potential range of 0.0-8.0 V in PBS buffer solution containing 1 mM of each glucose, cholesterol and urea (Fig. S4). From the figure, it is shown that the current is substantially enhanced and reaches to an optimum value at a certain potential. Such increase in current response is considered to be due to the enzymatic reactions with the analyte (i.e., glucose, cholesterol and urea). We found that working gate potential range for all the enzymes are different, which is due to the difference in enzymes characteristic including catalytic behavior towards specific analyte. Importantly, the increased currents were found to be in the potential range of 0-2, 0-3 and 0-6 V for glucose, cholesterol and urea, respectively. However, the saturation potential range was increased with increasing concentration of analytes. This confirms that the saturation was due to less amount of analyte and not related to the saturation of enzyme.

**Fig. S4**  $I_D$ - $V_G$  responses of ZnO NRs i-FETs array biosensor with 1 mM of each glucose, cholesterol and urea in 0.05 M PBS buffer solution.

Then, the change in pH with increasing concentrations of analyte in PBS (pH 7.4) was measured as it is well-known that the highly acidic (below pH 2) or strongly basic (above pH 8) environment can lead the fatal loss of enzymatic activity.<sup>2</sup>



Interestingly, a minor change (increased  $\sim 0.25$ ) in the pH was observed up to 90 mM of analyte concentrations (Fig. S5). This confirms that the above-prepared solutions can be reliably used for the detection of glucose, cholesterol and urea without having any effect of pH on the biosensor performances.

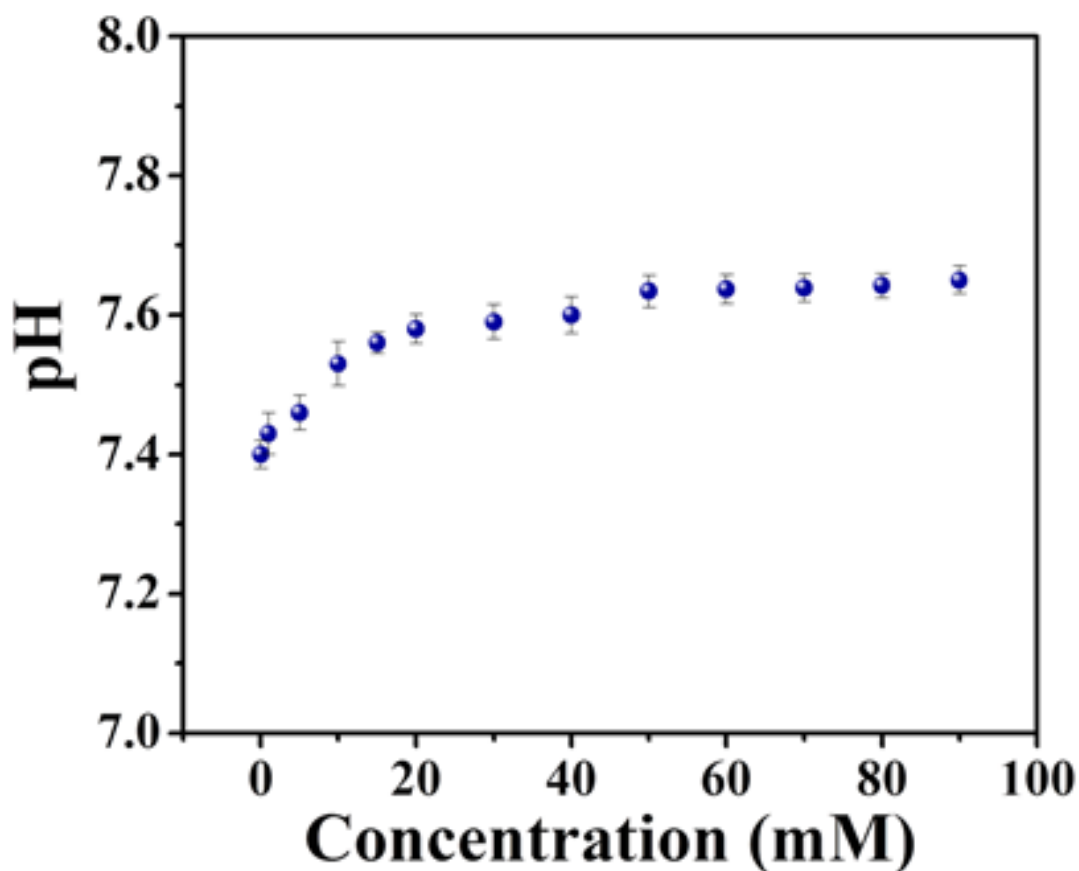


**Fig. S5** pH measurements as a function of analyte concentration.

Finally, the effect of pH on the fabricated ZnO NRs i-FETs biosensor was examined in the pH range of 5.0 - 9.0 at fixed concentrations of glucose, cholesterol and urea (Fig. S6). The optimum pH for the ZnO modified sensing arrays was noticed in the range 6.5 - 8.0. The rise and fall in sensor responses were attributed to the pH effect on the affinity of enzymes on substrate and higher enzyme stability in immobilized state. Also, it is presumed that if there were more hydrogen ions ( $H^+$ ) in the solution than the enzyme was designed for, these  $H^+$  ions would compete for

cationic binding sites present on enzyme thereby reduces the enzyme bioactivity. Likewise, if there were few H<sup>+</sup> ions in the solution, the same interactions would be disrupted by the relatively high concentration of hydroxide ions that lowers the enzyme bioactivity and ultimately abates biosensor sensitivity.

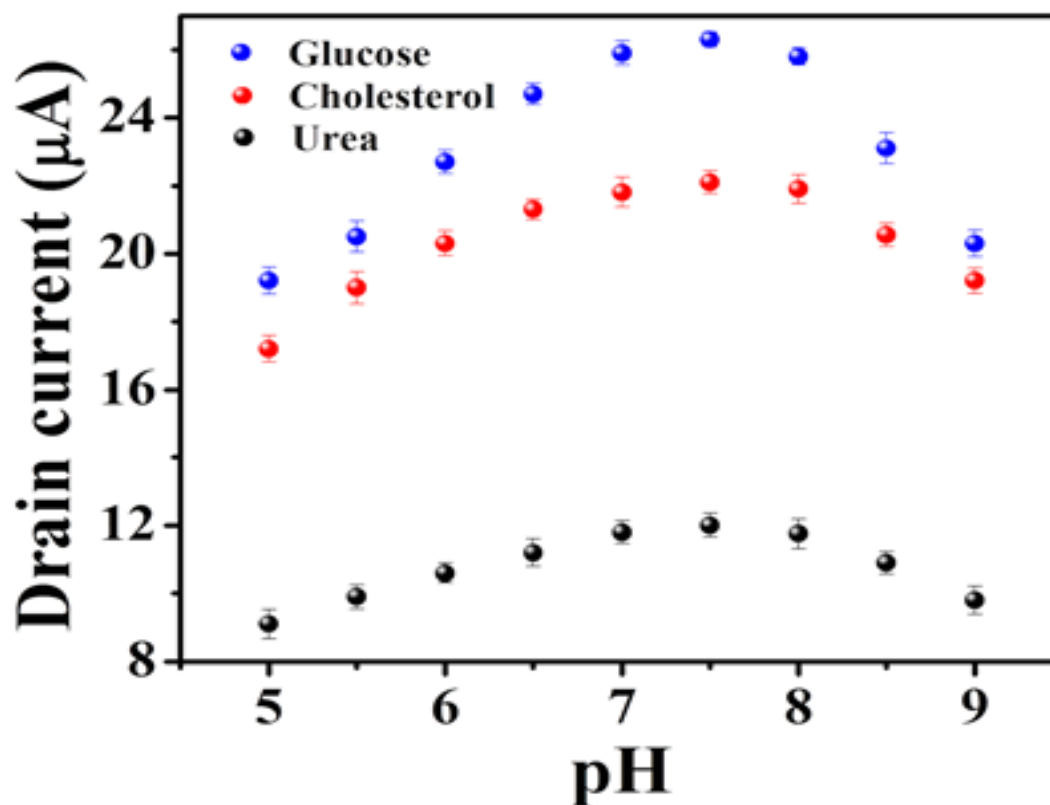


**Fig. S6** Effect of pH on the current responses of the ZnO NRs i-FETs array biosensor in 0.05 M PBS buffer in the range of 5.0-9.0 pH.

## 5. Selectivity test

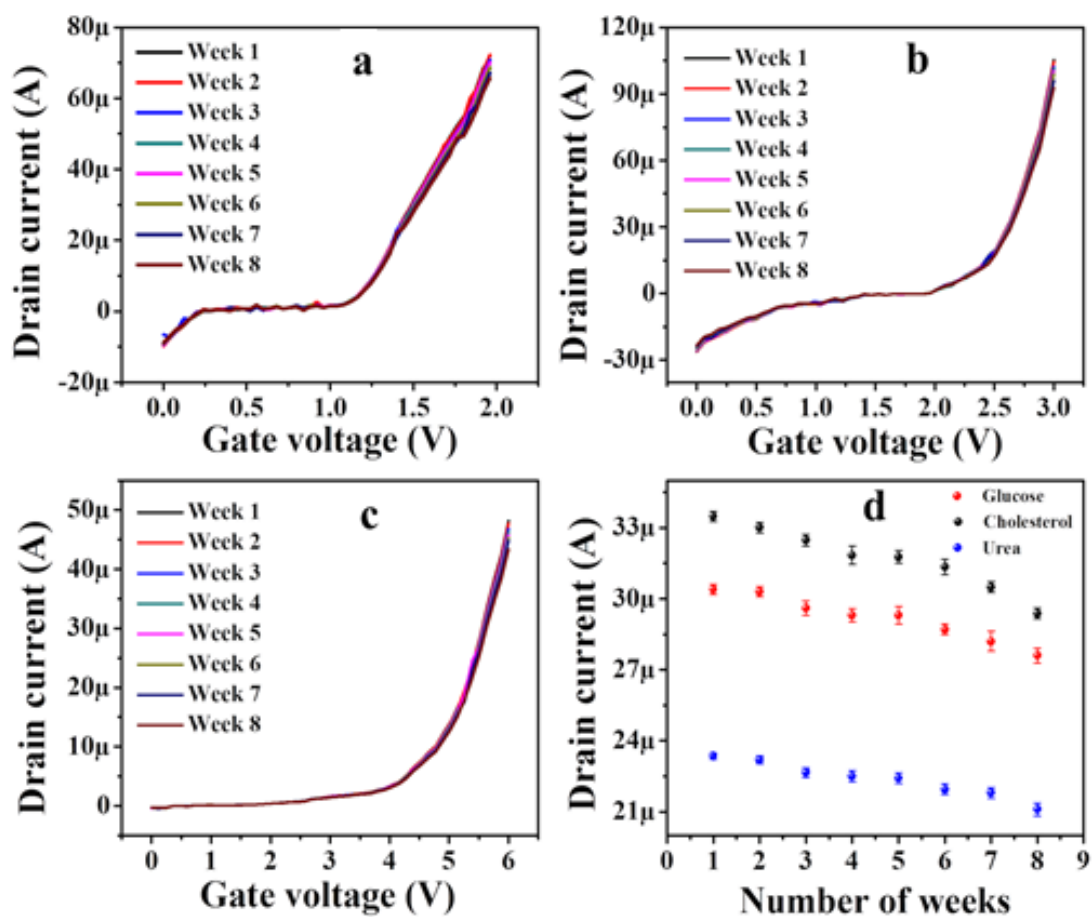


**Fig. S7**  $I_D$ - $V_G$  response of ZnO NRs i-FETs array biosensor in 0.05 M PBS buffer with 5 mM of each glucose, cholesterol and urea (a-c), and calibrated plot showing current response vs. number of usage week (d).

## 6. Stability test

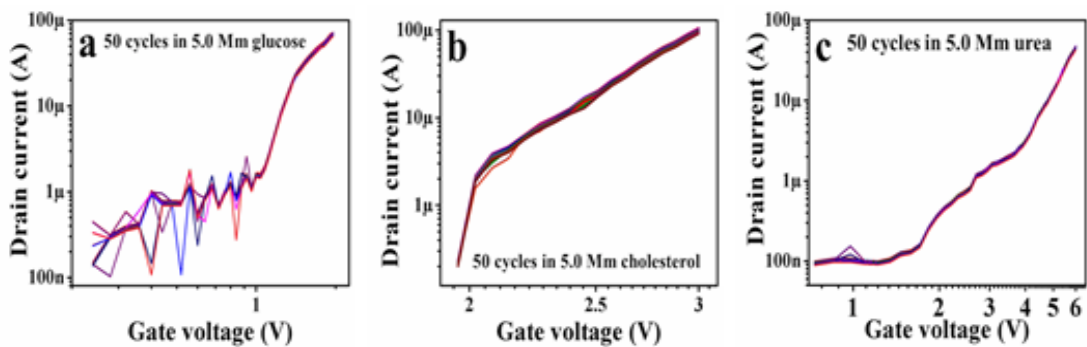


**Fig. S8**  $I_D$ - $V_G$  response of ZnO NRs i-FETs array biosensor in log scale for 50 cycles in 0.05 M PBS buffer with 5 mM of each glucose, cholesterol and urea (a-c).

## 7. Mice whole blood samples analysis

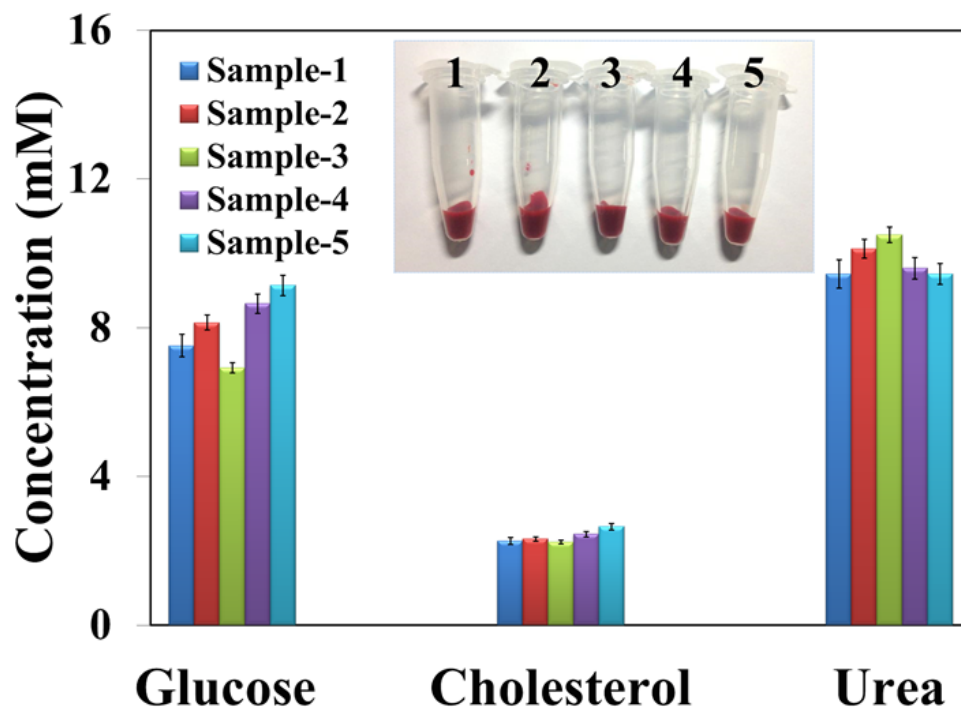


**Fig. S9** Determination of glucose, cholesterol and urea in mice whole blood samples. Insert photo image shows the mice whole blood samples. Error bars show the standard deviation for three different measurements.

## 8. Diabetic dog blood samples analysis

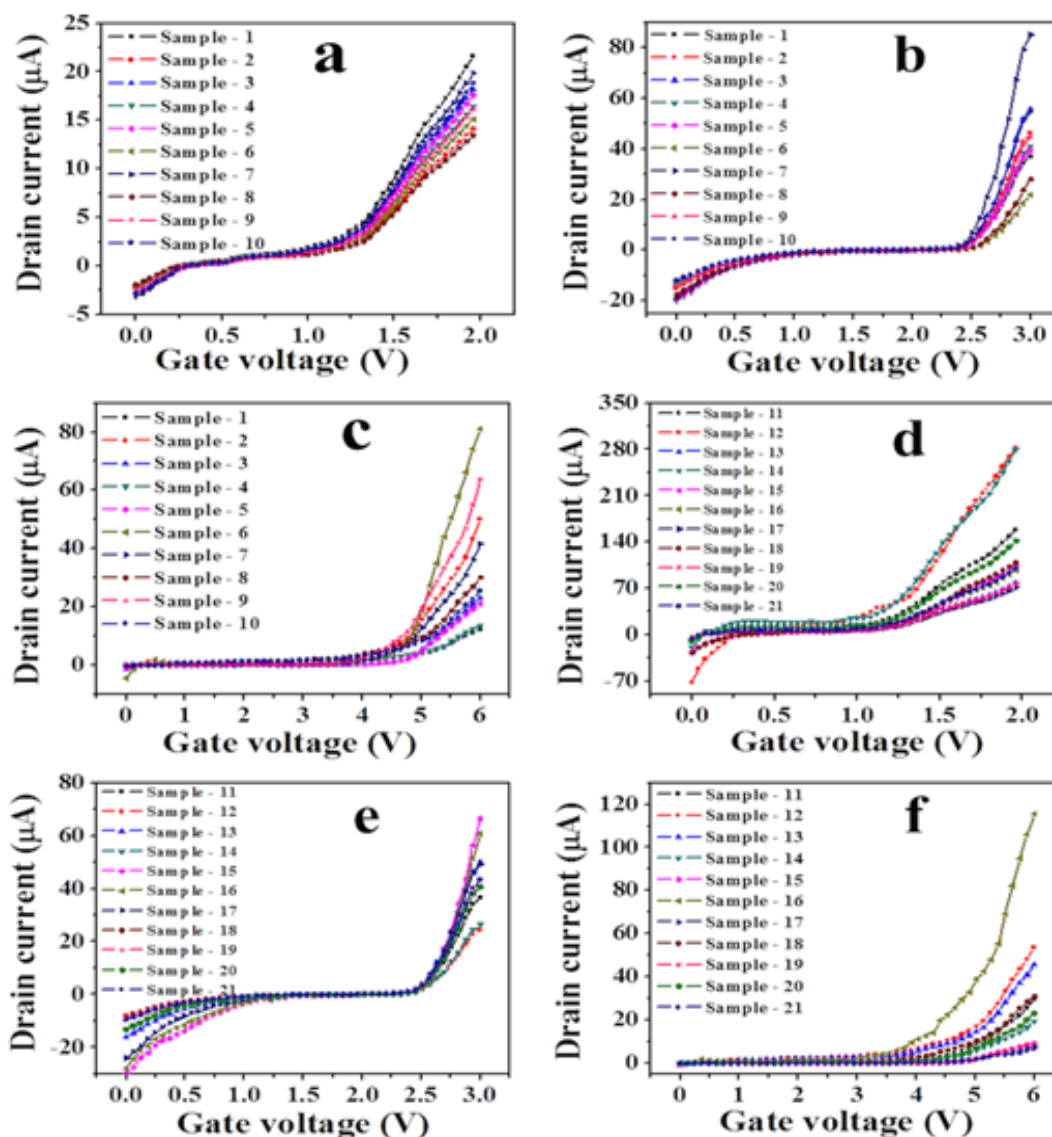


**Fig. S10**  $I_D$ - $V_G$  plots for determining analytes concentrations in diabetic dog patients. Collected blood samples from hypoglycemic (sample 1-10) and hyperglycemic (sample 11-21) dogs and filtered serum samples without any further dilution were used for the determinations of glucose, cholesterol and urea.

**Table S1.** Determination of glucose, cholesterol and urea concentrations in mice whole blood samples by the ZnO NRs i-FETs array biosensor with comparison between determined results and analytically measured data.

S.N.	Glucose		Cholesterol		Urea	
	ZnO NRs i-FETs biosensor	Analytical method	ZnO NRs i-FETs biosensor	Analytical method	ZnO NRs i-FETs biosensor	Analytical method
1	$7.52 \pm 0.31$	7.46	$2.27 \pm 0.09$	2.23	$9.45 \pm 0.38$	9.52
2	$8.14 \pm 0.20$	8.17	$2.32 \pm 0.06$	2.36	$10.12 \pm 0.33$	10.18
3	$6.92 \pm 0.26$	6.98	$2.24 \pm 0.07$	2.26	$10.5 \pm 0.41$	10.45
4	$8.65 \pm 0.34$	8.58	$2.45 \pm 0.08$	2.48	$9.60 \pm 0.37$	9.72
5	$9.14 \pm 0.32$	9.16	$2.65 \pm 0.10$	2.61	$9.45 \pm 0.36$	9.61

**Table S2.** Determination of glucose, cholesterol and urea concentrations in hypo- and hyperglycemic dog serum samples by the ZnO NRs i-FETs array biosensor with comparison between determined results and analytically measured data.

S. N.	Glucose		Cholesterol		Urea	
	ZnO NRs i-FETs biosensor	Analytical method	ZnO NRs i-FETs biosensor	Analytical method	ZnO NRs i-FETs biosensor	Analytical method
1	3.52 ± 0.13	3.56	3.45 ± 0.11	3.44	3.22 ± 0.12	3.17
2	2.29 ± 0.08	2.33	4.27 ± 0.06	4.32	12.63 ± 0.43	12.96
3	2.89 ± 0.15	3.0	5.23 ± 0.14	5.29	6.02 ± 0.10	5.99
4	2.75 ± 0.11	2.72	3.72 ± 0.15	3.83	3.52 ± 0.15	3.56
5	2.92 ± 0.10	3.0	3.68 ± 0.08	3.65	5.50 ± 0.19	5.49
6	2.48 ± 0.05	2.5	2.02 ± 0.07	2.04	21.52 ± 0.82	21.06
7	3.21 ± 0.08	3.27	7.87 ± 0.19	7.97	10.45 ± 0.32	10.81
8	2.24 ± 0.04	2.22	2.62 ± 0.13	2.67	7.62 ± 0.09	7.78
9	2.62 ± 0.17	2.66	4.18 ± 0.11	4.12	16.47 ± 0.28	16.72
10	3.04 ± 0.16	3.0	5.11 ± 0.21	5.13	6.52 ± 0.21	6.57
11	20.27 ± 0.56	19.11	3.42 ± 0.23	3.46	7.68 ± 0.43	7.72
12	34.37 ± 1.03	34.05	2.28 ± 0.18	2.24	13.92 ± 0.54	13.88
13	9.52 ± 0.32	9.39	4.67 ± 0.12	4.69	11.45 ± 0.63	11.82
14	33.28 ± 0.71	33.83	2.52 ± 0.09	2.46	4.72 ± 0.33	4.99
15	12.12 ± 0.27	12.28	6.22 ± 0.26	6.21	3.37 ± 0.11	3.42
16	11.84 ± 0.29	11.72	5.67 ± 0.33	5.72	29.32 ± 1.28	30.0
17	8.52 ± 0.23	8.56	4.63 ± 0.25	4.58	2.04 ± 0.05	1.96
18	13.32 ± 0.43	13.05	4.93 ± 0.26	4.90	8.12 ± 0.18	8.03
19	9.17 ± 0.15	9.22	3.82 ± 0.23	3.87	2.45 ± 0.07	2.38
20	17.14 ± 0.19	17.05	4.05 ± 0.21	3.97	5.92 ± 0.23	5.99
21	12.11 ± 0.21	12.0	6.12 ± 0.31	6.14	1.68 ± 0.14	1.64

## Reference

1. J. C. Claussen, A. D. Franklin, A. Haque, D. M. Porterfield and T. S. Fisher, *ACS Nano*, 2009, **3**, 37.
2. R. Wilson and A. P. F. Turner, *Biosens. Bioelectron.*, 1992, **7**, 165.